JOURNAL OF SOLID STATE CHEMISTRY 97, 443–451 (1992)

A TEM Study of the Ordering of Excess Interstitial Oxygen Atoms in $Ln_2NiO_{4+\delta}$ (Ln = La, Nd)

L. C. OTERO-DIAZ,*[,1] A. R. LANDA,* F. FERNANDEZ,*
R. SAEZ-PUCHE,* R. WITHERS,† AND B. G. HYDE†

Departamento de Quimica Inorganica, Facultad de Ciencias Quimicas, Universidad Complutense de Madrid, Madrid 28040, Spain; and †Research School of Chemistry, Australian National University, GPO Box 4, Canberra, ACT, 2601, Australia

Received September 25, 1991

A Transmission Electron Microscope (TEM) study of the oxygen excess $Ln_2NiO_{4+\delta}$ (Ln = La, Nd) compounds shows long range ordering of interstitial oxygen, characterized by weak superlattice reflections whose modulation wave-vector can be both commensurate as well as incommensurate with respect to the reciprocal lattice of the basic K_2NiF_4 structure type for both oxides. The excess interstitial oxygen atoms are sometimes found to be rather mobile and susceptible to electron beam irradiation, although less so in the case of the Nd compound. A new type of superstructure has been found in the Nd case, and a model for the oxygen interstitial ordering is given.

1. Introduction

The effect of excess oxygen and its influence upon the structure and physical properties of $Ln_2MO_{4+\delta}$ materials (Ln = La, Pr, Nd; M = Cu, Ni, Co) have recently been subjects of great interest (*1*, *2*). This has largely been due to the finding that excess interstitial oxygen atoms inject holes into CuO_2 sheets of the M = Cu compounds and lead to them becoming superconducting (*3*, *4*). It was initially thought (*5*) that this may also have been the case for the M = Ni compounds, but more recent measurements suggest that superconductivity does not occur in these latter materials (*6*). Nevertheless the crystal chemistry underlying the existence of oxygen interstitials in this family of materials and the ordering thereof remain a fascinating subject for study. According to powder and single crystal neutron diffraction studies (*7–9*), the excess oxygen atoms are located between two adjacent LaO layers at interstitial sites tetrahedrally coordinated by La atoms and lead to a substantial distortion (~0.5 Å) of the structure in their immediate vicinity.

Brown (*10*) has recently analyzed the rich crystal chemistry of $La_2NiO_{4+\delta}$ in terms of the bond length–bond valence approach. He has shown that the two structural phase transformations (involving shifts away from the high symmetry K_2NiF_4-type parent structure) which experimentally occur upon lowering temperature for the stoichiometric material (*4*) (δ = 0)

[1] To whom correspondence should be addressed.

0022-4596/92 $3.00

can be understood in terms of a two-dimensional lattice mismatch between the LnO and MO_2 layers. The observed lattice parameters for the $Ln_2MO_{4+\delta}$ materials are always such that the Ln atoms are underbonded and the M atoms overbonded (*10*) for the ideal, high symmetry K_2NiF_4-type parent structure. The stoichiometric materials ($\delta = 0$) compensate for this mismatch by a coupled rotation and expansion of the MO_6 octahedra. This simultaneously reduces the Apparent Valence (AV) of the M cation as well as increases that of the Ln atom. Brown (*10*) has also used the bond length–bond valence approach to show that the nonstoichiometric materials (δ not equal to 0) can achieve a similar effect via the insertion of oxygen interstitials between adjacent LnO layers and subsequent relaxation. A possible model for the ordering of the interstitial oxygen atoms in $Ln_2NiO_{4+\delta}$ ($\delta = \frac{1}{6}$) was proposed (*10*).

Ordering of these interstitial oxygen atoms and the subsequent structural relaxation leads to rather weak extra satellite reflections (at $\mathbf{G} \pm m\mathbf{q}$, m an integer) in addition to the strong matrix reflections (at $\mathbf{G}$) characteristic of the underlying, K_2NiF_4-related average structure. These weak extra satellite reflections are most detected by electron diffraction. The first TEM study of oxygen interstitial ordering in this family of materials was recently reported for $La_2NiO_{4+\delta}$ by Hiroi *et al.* (*11*). Two types of homologous series of superstructures were found and probable ordering schemes proposed. Neither was in agreement with that proposed by Brown (*10*). It was also mentioned that the interstitial oxygen atoms were rather mobile, and hence the observed superstructures could be easily altered by excess electron beam irradiation. The purpose of this paper is to present the results of a TEM study of oxygen interstitial ordering in $Ln_2MO_{4+\delta}$ materials. In the case of $Nd_2NiO_{4+\delta}$, the observed superstructures are found to be rather more stable to electron beam irradiation than the corresponding La and Pr compounds.

2. Experimental Methods

Sample Preparation

The $Ln_2NiO_{4+\delta}$ oxides were prepared by heating stoichiometric amounts of high purity La_2O_3 or Nd_2O_3 (99.99%) with NiO (99.99%) in air at 1623 K for 72 hr with two interruptions for grinding. La_2O_3 was preheated overnight at 1273 K in air to remove moisture and CO_2. The black powders were annealed in a stream of O_2 at 773 K for 24 hr and then slowly cooled (over 6 hr) to room temperature under the oxygen flow.

Diffraction Studies

The $La_2NiO_{4+\delta}$ sample was examined by X-ray powder diffraction, using a Siemens K 810 diffractometer with Cu$K\alpha$ radiation, and a D-501 goniometer provided with a secondary graphite monochromator. The data were analyzed by using the Rietveld refinement method. For the electron microscopy/diffraction studies both samples were ground under ethanol, dispersed on Cu grids coated with holey-carbon support films, and examined in a JEOL 2000FX and a JEOL 4000EX, both fitted with goniometer stages.

3. Experimental Results

3.1 X-ray Diffraction

The refined unit cell parameters for the $La_2NiO_{4+\delta}$ samples were

$a = 3.8619$ Å, $c = 12.688$ Å, Space group $I4/mmm$; $V = 189.20(4)$ Å^3.

These values are in good agreement with those previously reported (*7*).

3.2 Electron Diffraction/Microscopy

All diffraction patterns have been indexed with respect to an underlying, $I4/mmm$,

$a = b \sim 3.85$ Å, $c \sim 12.5$ Å, K_2NiF_4-type average structure.

(*i*) *$La_2NiO_{4+\delta}$*. Hiroi *et al.* (*11*) reported two different types of homologous series of superstructures along with most probable oxygen interstitial ordering schemes for them. The first homologous series was reported to be characterized by one-dimensional arrays of superlattice spots along a {011}* direction of reciprocal space (note that (*hkl*)* refers to the reciprocal lattice vector $h\mathbf{a}^* + k\mathbf{b}^* + l\mathbf{c}^*$ in what follows) with an interval $1/n$th of the {011}* length (see Fig. 1(a) and (b) of Hiroi *et al.* (*11*) for $n = 2$ and 3). Analysis of Hiroi *et al.*'s oxygen interstitial ordering scheme for this type of homologous series (see Fig. 4 of Hiroi *et al.* (*11*) shows that the corresponding reciprocal lattice should be characterized by reflections of the form $\mathbf{G} \pm m\mathbf{q}_{\text{prim.}}$, where **G** corresponds to the strong matrix reflections characteristic of the underlying, K_2NiF_4-type average structure, m is an integer, and where the primary modulation wave-vector, $\mathbf{q}_{\text{prim.}}$, characteristic of the oxygen interstitial ordering, is given by

$$\mathbf{q}_{\text{prim.}} = \tfrac{1}{2}\mathbf{a}^* + \tfrac{1}{4}\mathbf{b}^* - \tfrac{1}{4}\mathbf{c}^* \quad \text{for } n = 2$$

and by

$$\mathbf{q}_{\text{prim.}} = \tfrac{1}{2}\mathbf{a}^* + \tfrac{1}{3}\mathbf{b}^* - \tfrac{1}{6}\mathbf{c}^* \quad \text{for } n = 3.$$

The $\mathbf{q} = 1/n\,(\mathbf{b}^* + \mathbf{c}^*)$ satellites shown in Figs. 1(a) and (b) of Hiroi *et al.* (*11*) are not therefore first-order but second-order satellite reflections, i.e., $\frac{1}{2}(011)^*$ can be written as $\mathbf{G} + 2\mathbf{q}_{\text{prim.}}(n = 2)$. Given *I4/mmm* parent symmetry, note that there are 8 symmetry-equivalent $\mathbf{q}_{\text{prim.}}$-vectors, namely $\frac{1}{2}\mathbf{a}^* \pm \frac{1}{4}\mathbf{b}^* \pm \frac{1}{4}\mathbf{c}^*$ and $\pm\frac{1}{4}\mathbf{a}^* + \frac{1}{2}\mathbf{b}^* \pm \frac{1}{4}\mathbf{c}^*$. If only one of these symmetry-equivalent $\mathbf{q}_{\text{prim.}}$-vectors is ever present in any one local area, then the resultant space group symmetry is, of necessity, lowered to triclinic. Careful observation and tilting experiments show that this is indeed the case. Thus one should expect, and experimentally we observe, distinct twin variants for each n and corresponding $\mathbf{q}_{\text{prim.}}$. Our results for this type of homologous series of superstructure thus confirm the results of Hiroi *et al.* (*11*). We could not, however, detect any induced triclinic strain in the underlying K_2NiF_4-type average structure cell dimensions. Jorgensen *et al.* (*7*) noted that their $La_2NiO_{4.18}$ specimen, while it appeared to index on a tetragonal, $a = b \sim 3.856$ Å, $c \sim 12.664$ Å, *I4/mmm* cell, was in fact very slightly orthorhombic, $a = 5.4469$, $b = 5.4569$, $c = 12.6637$ Å, *Fmmm*.

The sensitivity of the oxygen interstitial ordering in $La_2NiO_{4+\delta}$ to electron beam irradiation has also been studied. Figure 1, for example, shows a series of [100] zone axis SADPs taken from exactly the same area of specimen. In (a), it would appear that only the strong matrix reflections **G** characteristic of the underlying K_2NiF_4-related average structure occur. Close observation of the negative, however, shows a very weak diffuse distribution (too weak to reproduce in the figure). After focusing the beam on the specimen for ~2 mins, the SADP shown in (b) was obtained. Clearly the illuminated area (~0.5 μm in diameter) now contains domains of $n = 2$ (two different twin-related variants) and one $n = 3$ variant (the different types of satellite reflections have been marked by arrows in (b)). After observation for a few more minutes, the SADP shown in (c) was obtained. Now twin-related variants are visible for both $n = 2$ and $n = 3$. After a few more minutes, the SADP shown in (d) was obtained. Now the $n = 3$ variants have disappeared but two twin-related, $n = 2$ variants remain (one stronger than the other). In Fig. 1(e), a low magnification Bright Field (BF) image is shown from this same area. Twin boundaries perpendicular to **c** separating the two twin-related, $n = 2$ variants are clearly visible. Along the edge of the crystal, a regular array of defect contrast can be seen. These defects were observed to be rather mobile under electron beam irradiation. In addition, the beginnings

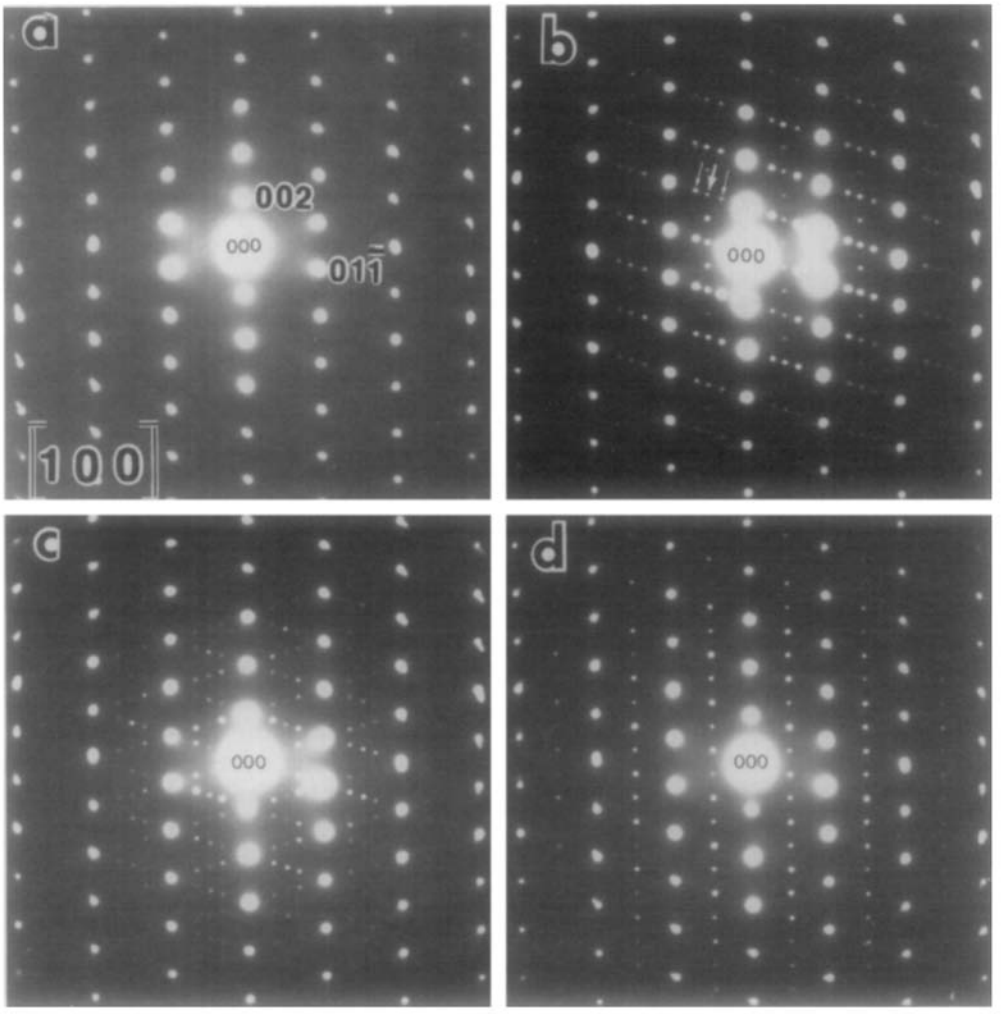

FIG. 1. (a), (b), (c), (d), and (f). [100] zone axis SADPs of $La_2NiO_{4+\delta}$ taken from exactly the same area of specimen showing the effect of electron beam irradiation upon reciprocal space; (e) is a Bright Field image taken just after the SADP shown in (f). Indexing of diffraction patterns is always with respect to the reciprocal lattice of the K_2NiF_4 parent structure.

of characteristic defect fault planes (arrowed) perpendicular to the **c**-axis in the underlying K_2NiF_4-related parent structure can be seen growing in from the crystal edge. Fig. 1(f) shows the SADP obtained from the same area immediately prior to the recording of the image shown in Fig. 1(e). The streaking of the parent reflections along **c*** characteristic of this planar faulting is observed along with the satellite spots characteristic of the $n = 2$ twin variants. The streaking of the parent reflections along **c*** in SADPs from other orientations rotated around **c** appears to show an alternation characteristic of body-centering in the fault structure. Finally, it should be pointed out that incommensurate ordering of this type is also often observed. In the [100] zone axis

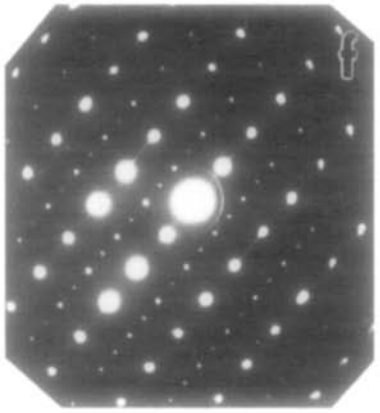

FIG. 1—*Continued*

SADP of Fig. 2, for example, second-order incommensurate satellite reflections can be seen canted very slightly away from a {011}* direction, i.e., the corresponding primary modulation wave-vector is no longer commensurate with the underlying parent structure.

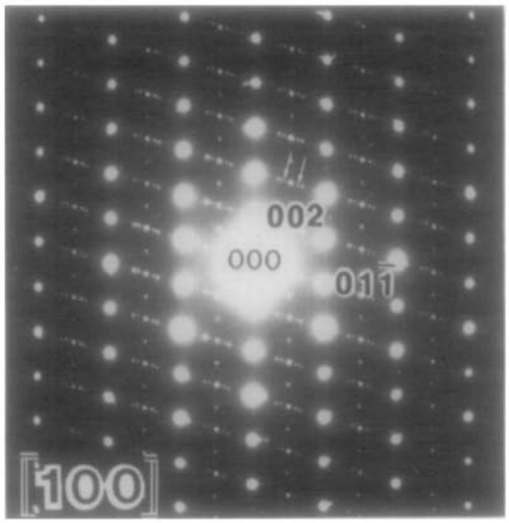

FIG. 2. [100] zone axis SADP from a crystal of $La_2NiO_{4+\delta}$ showing incommensurate satellite reflections (arrowed) for the first type of homologous series.

The second type of homologous series reported by Hiroi *et al.* (*11*) (their Fig. 1(c)) can be characterized by satellite reflections of the form $\mathbf{G} \pm m\mathbf{q}_{\text{prim.}}$, where the primary modulation wave-vector can be chosen to be $\mathbf{q}_{\text{prim.}} = \frac{1}{4}\mathbf{a}^* \pm \frac{3}{4}\mathbf{b}^*$ or $\mathbf{q}_{\text{prim.}} = \frac{3}{4}\mathbf{a}^* \pm \frac{1}{4}\mathbf{b}^*$. Only one of these $\mathbf{q}_{\text{prim.}}$-vectors, however, is ever locally present. Thus one should expect, and experimentally we observe, twin variants. Figure 3, for example, shows a typical [110] zone axis SADP characteristic of this second type of homologous series. Note that $\frac{1}{4}(114)^* = \frac{1}{4}\mathbf{a}^* - \frac{3}{4}\mathbf{b}^* + (\mathbf{b}^* + \mathbf{c}^*) = \frac{1}{4}\mathbf{a}^* - \frac{3}{4}\mathbf{b}^* + \mathbf{G}$. The extra satellite reflections at $\mathbf{G} \pm \frac{1}{2}(112)^*$ present in Fig. 3 but not present in Fig. 1(c) of Hiroi *et al.* (*11*) correspond to the second harmonic satellites of another twin variant. Only the possible primary modulation wave-vectors listed above were ever observed for this second type of superlattice.

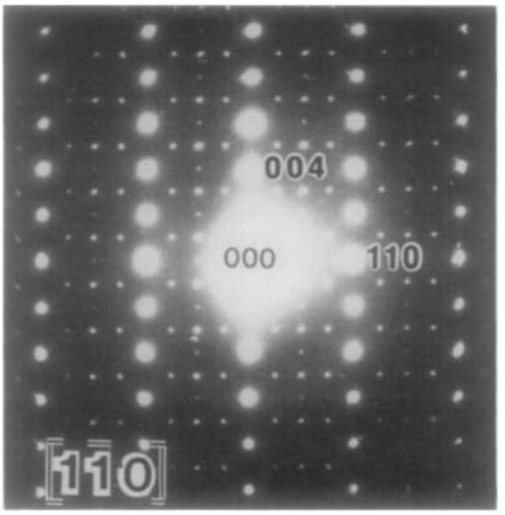

FIG. 3. [1, −1,0] zone axis SADP from a crystal of $La_2NiO_{4+\delta}$ showing the satellite reflections characteristic of the second type of homologous series reported in Ref. (*11*).

It is important to remark that the extra satellite reflections characteristic of oxygen interstitial ordering were only observed when using a JEOL 2000FX microscope but not when using the higher resolution JEOL 4000EX microscope, presumably because of harsher reducing conditions in the latter microscope leading to the nonreversable removal of all the interstitial oxygen atoms from the sample. Indeed, even in the case of the JEOL 2000FX microscope, it was sometimes possible to clearly detect a worsening of the microscope vacuum upon electron irradiation! Given this sensitivity of the samples to electron beam irradiation, it is clearly not possible to say anything very precise as regards the stoichiometry of any particular grain of material examined in the TEM.

(*ii*) *$Nd_2NiO_{4+\delta}$*. It was found that the oxygen ordering giving rise to the extra satellite reflections is more stable to electron beam irradiation in this case than for the $La_2NiO_{4+\delta}$ case. By far the most commonly observed superstructure in the case of $Nd_2NiO_{4+\delta}$ is characterized by weak satellite reflections of the form $\mathbf{G} \pm m\mathbf{q}_{\text{prim.}}$, where the primary modulation wave-vector is given by $\mathbf{q}_{\text{prim.}} = \frac{3}{8}\mathbf{a}^* + \frac{1}{8}\mathbf{b}^* + \mathbf{c}^*$ (see Fig. 4). Again there are 8 symmetry-equivalent $\mathbf{q}_{\text{prim.}}$-vectors. Careful tilting experiments, however, again demonstrate that only one of these 8 symmetry-equivalent $\mathbf{q}_{\text{prim.}}$-vectors is ever present in any given local area. Thus the resultant space group symmetry is of necessity lowered to monoclinic. Note that there also exist weak satellite reflections at $\mathbf{G} \pm m/4(114)^*$ in Fig. 4. These correspond to second harmonic satellite reflections of the twin variant with primary modulation wave-vector $\frac{1}{8}\mathbf{a}^* - \frac{3}{8}\mathbf{b}^* + \mathbf{c}^*$.

The most probable ordering scheme of the oxygen interstitials corresponding to this diffraction information is given in Fig. 5

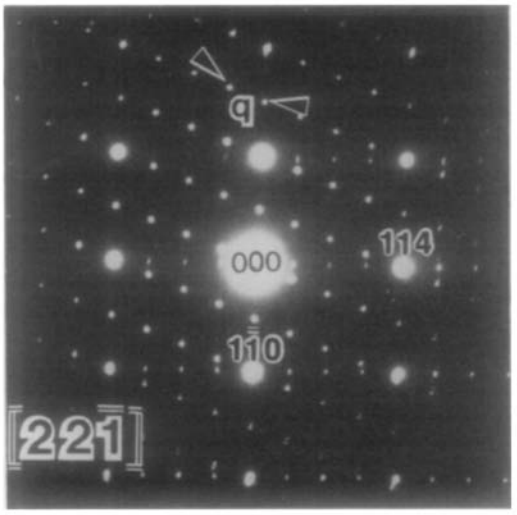

FIG. 4. A typical [2,2, −1] zone axis SADP showing the characteristic $\mathbf{G} \pm m\mathbf{q}_{\text{prim.}}$ satellite reflections (where the primary modulation wave-vector is given by $\mathbf{q}_{\text{prim.}} = \frac{3}{8}\mathbf{a}^* + \frac{1}{8}\mathbf{b}^* + \mathbf{c}^*$) most commonly observed in the $Nd_2NiO_{4+\delta}$ specimen. The indexing of the strong reflections is always with respect to the reciprocal lattice of the K_2NiF_4 parent structure.

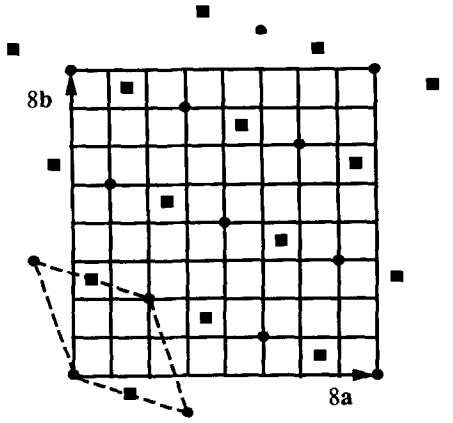

FIG. 5. Shows the most probable interstitial oxygen ordering scheme compatible with the superstructure shown in Fig. 4. Filled circles and squares represent oxygen interstitials at heights of 0 and $\frac{1}{2}$, respectively.

(corresponding to a δ of $\frac{1}{8}$ and a $\mathbf{q}_{\text{prim.}}$ of $\frac{3}{8}\mathbf{a}^* + \frac{1}{8}\mathbf{b}^* + \mathbf{c}^*$). Only the oxygen interstitials are shown (see Ref. (*7*) or Fig. 1 of Brown (*10*) for the interstitial positions with respect to the parent structure). The filled circles correspond to oxygen interstitials at $z = 0$, while the filled squares correspond to oxygen interstitials at $z = \frac{1}{2}$. The $(3\mathbf{a}^* - \mathbf{b}) \times (-\mathbf{a} + 3\mathbf{b}) \times \mathbf{c}$ resultant monoclinic supercell is shown by the dashed lines.

As for the $La_2NiO_{4+\delta}$ sample, twinning was commonly observed, as shown in Fig. 6(a). In Fig. 6(b) we present a high resolution image within one of these twin domains, taken down the [−5,5,1] zone axis, showing both lattice fringes corresponding to the K_2NiF_4 parent structure as well as the ~7.5 Å fringes (arrowed) corresponding to the oxygen interstitial superstructure (In fact, the primary modulation wave-vector $\mathbf{q}_{\text{prim.}} = \frac{3}{8}\mathbf{a}^* + \frac{1}{8}\mathbf{b}^* + \mathbf{c}^*$ is not quite excited at this zone axis so that the superstructure fringes are not quite edge on. One would need to tilt ~3° to the [−5,5,1.25] direction for the superstructure fringes to be exactly edge on).

As also occurred for the $La_2NiO_{4+\delta}$ material, more than one type of ordering pattern could sometimes be observed (see the SADPs shown in Figs. 7(a) and 7(b)). Rather more rarely, characteristic diffuse intensity distributions instead of sharp satellite reflections could be observed.

Conclusions

We have presented the results of a TEM study of the oxygen interstitial ordering present in the $La_2NiO_{4+\delta}$ and $Nd_2NiO_{4+\delta}$ systems. The weak satellite reflections characteristic of such ordering have been very difficult to detect by X-ray and neutron scattering (see Ref. (*7*) and (*8*)) but are clearly visible in electron diffraction patterns. The reciprocal lattices of the most commonly observed superlattices are described in both cases. For $La_2NiO_{4+\delta}$ our results essentially confirm those of Hiroi *et al.* (*11*). In the case of $Nd_2NiO_{4+\delta}$, a new type of superlattice ordering $((3\mathbf{a} - \mathbf{b}) \times (-\mathbf{a} + 3\mathbf{b}) \times \mathbf{c}$ and characterized by the primary molulation wave-vector $\mathbf{q}_{\text{prim.}} = \frac{3}{8}\mathbf{a}^* + \frac{1}{8}\mathbf{b}^* + \mathbf{c}^*$) has been observed and a possible ordering scheme proposed. It is shown that electron beam irradiation can sometimes have a marked effect upon the diffraction patterns observed, i.e., the interstitial oxygens are clearly mobile, especially in the $La_2NiO_{4+\delta}$ case. Thus it is perhaps not surprising that a range of (incommensurate, commensurate, and even diffuse) satellite reflections can sometimes be observed.

Acknowledgments

We thank the Centro de Microscopia Electronica (Universidad Complutense de Madrid) for facilities. One of us, B.G.H., thanks the D.G.I.C.Y.T. (Secretaria de Estado de Universidades e Investigacion, M. E. y C.) for a sabbatical visiting professorship in 1990. This research was supported by the CYCIT project MAT 89-0768.

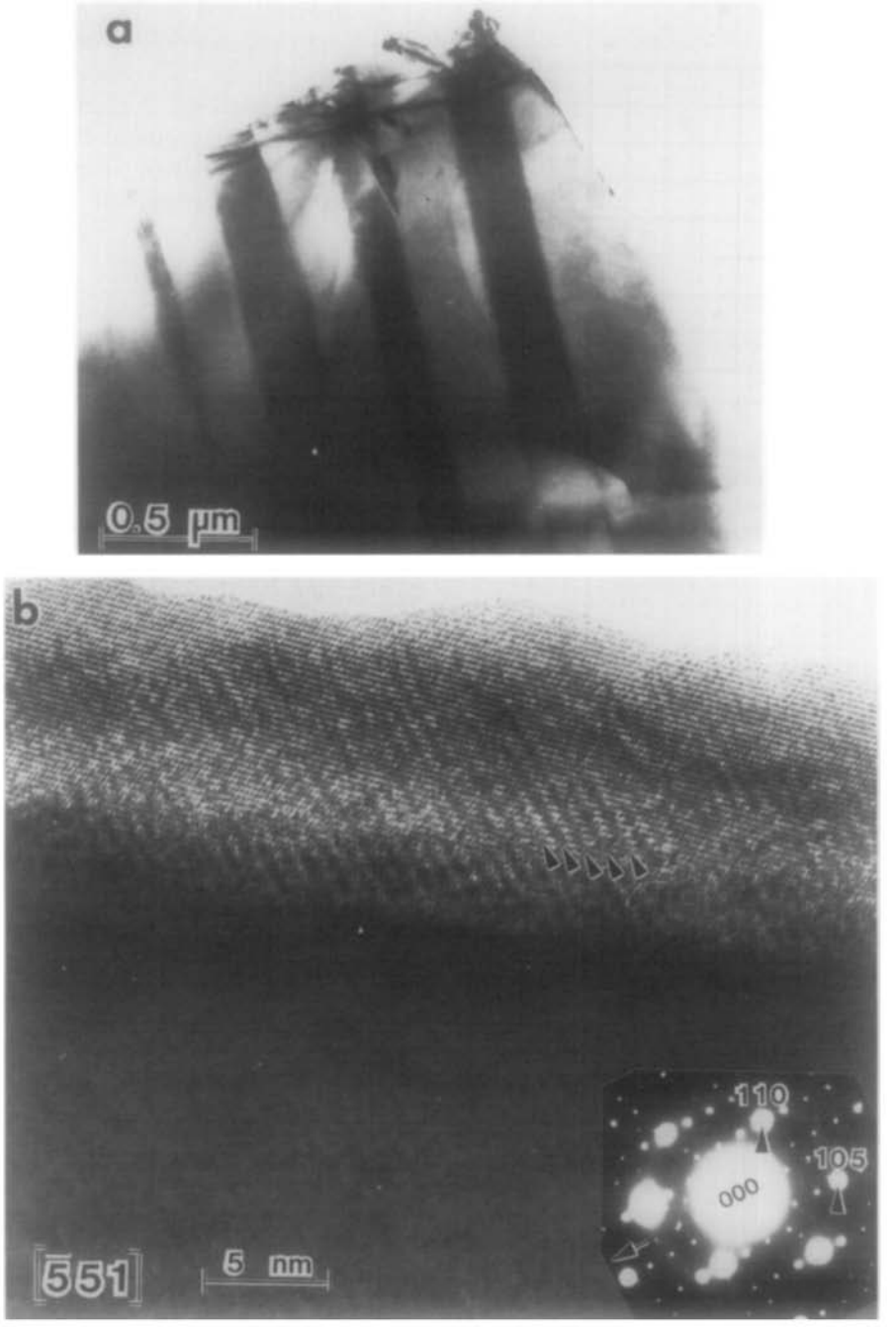

FIG. 6. (a) Low magnification image of twin variants in $Nd_2NiO_{4+\delta}$. (b) Shows a high resolution image taken within one of these twin domains down the [−5,5,1] zone axis showing both lattice fringes corresponding to the K_2NiF_4 parent structure as well as the ~7.5 Å fringes (arrowed) corresponding to the oxygen interstitial superstructure. The corresponding SADP is inset.

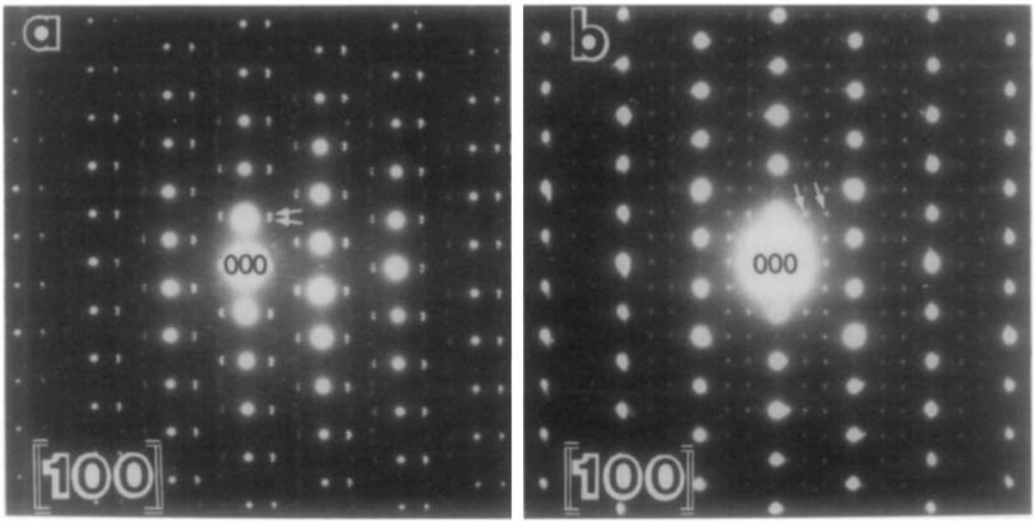

FIG. 7. [100] zone axis SADPs showing less-commonly observed types of ordering pattern occasionally seen in the $Nd_2NiO_{4+\delta}$ specimen.

References

1. P. GANGULY AND C. N. R. RAO, *J. Solid State Chem.* **53,** 193 (1984).
2. D. J. BUTTREY, P. GANGULY, J. M. HONIG, C. N. R. RAO, R. R. SCHARTMAN, AND G. N. SUBBANNA, *J. Solid State Chem.* **74,** 233 (1988).
3. J. BEILLE, R. CABANEL, G. CHAILLOUT, B. CHEVALIER, G. DEMAZEAU, F. DESLANDES, J. ETOURNEAU, P. LEJAY, C. MICHEL, J. PROVOST, B. RAVEAU, A. SULPICE, J. L. THOLENCE, AND R. TOUNIER, *C. R. Acad. Sci. Paris Ser. 2* (18) **304,** (1987).
4. J. D. JORGENSEN, B. DABROWSKI, S. PEI, D. G. HINKS, L. SODERHOLM, B. MOROSIN, J. E. SCHIRBER, E. L. VENTURINI, AND D. S. GINLEY, *Phys. Rev. B* **38,** 11337 (1988).
5. Z. KAKOL, J. SPALEK, AND J. M. HONIG, *Solid State Commun.* **71,** 283 (1989); **71,** 288 (1989); **71,** 511 (1989).
6. S. A. HOFFMAN, C. VENKATARAMAN, S. N. ERLICH, S. M. DURBIN, AND G. L. LIEDL, *Phys. Rev. B* **43,** 7852 (1991).
7. J. D. JORGENSEN, B. DABROWSKI, S. PEI, D. R. RICHARDS, AND D. G. HINKS, *Phys. Rev. B* **40,** 2187 (1989).
8. C. CHAILLOUT, S. W. CHEONG, Z. FISK, M. S. LEHMAN, M. MAREZIO, B. MOROSIN, AND J. E. SCHIRBER, *Physica C* **158,** 183 (1989).
9. J. RODRIGUEZ-CARVAJAL, M. T. FERNANDEZ-DIAZ, AND J. L. MARTINEZ, *J. Phys. Condens. Matter* **3,** 3215 (1991).
10. I. D. BROWN, *Z. Kristallogr.*, in press.
11. Z. HIROI, T. OBATA, M. TAKANO, Y. BANDO, Y. TAKEDA, AND O. YAMAMOTO, *Phys. Rev. B* **41,** 11665 (1990).